Impingement of Internal Waves from Below onto a Moving Mixed Surface Layer[1]

ERIK MOLLO-CHRISTENSEN

Department of Meteorology, Massachusetts Institute of Technology, Cambridge 02139

(Manuscript received 10 August 1976, in revised form 6 May 1977)

ABSTRACT

Discussion of the generation of internal waves by tidal flow over bottom topography concludes that isobath convergence has an important effect on wave intensity near the sea surface, and also predicts that all harmonics of the tide will be present in the emitted waves.

A simple analysis of the reflection of internal waves by a moving surface layer predicts that the surface layer disturbance will be amplified by, at the most, a factor of 2, and that this amplification is selective in wavenumber. For waves near inertial frequency, the impinging wave can excite disturbances that grow exponentially with time. Data from the GATE experiment show a clear tidal signal in isotherm depths near the thermocline and a possible inertial period variation as predicted by the simplified case analyzed.

1. Introduction

Rattray (1960) has described the generation of internal waves by tidal flow over topography. Halpern (1971) and later others have observed wave packets propagating over continental shelf areas. Recently obtained satellite data show that such waves are ubiquitous (Apel *et al.*, 1975).

During the GATE experiment, internal waves were observed by many of the participants, and were reported by Ostapoff (1975), Mollo-Christensen *et al.* (1975), Woods (1975), Siedler and Zenk (1975), Koblinsky and Grose (1975) and others.

The ship XBT data, analyzed by Grose (1976, personal communication), show that the isotherms tend to take a sudden dip once per tidal period. Ostapoff *et al.* (1975) suggest that the internal waves they observed were topographically generated at one of the seamounts on the Sierra Leone Rise, between 50 and 100 km from the point of observation.

There are of course many possible mechanisms for generation of internal waves. Among them are moving atmospheric pressure patterns, nonlinear resonant interaction between surface and internal waves (see Phillips, 1966), while convective instabilities caused by surface evaporation and cooling can be expected to cause convective overturning near the surface every sunny day and even for each cloud passage. In addition there are shear flow instabilities that, influenced by stratification and rotation, can occur and generate internal waves with a concomitant modification of the basic flow toward neutral stability. In fact, one should expect most naturally occurring flows to be near a state of neutral stability, since the Reynolds stresses associated with instability will tend to modify the mean flow toward a neutrally stable mean profile.

The apparent periodic occurrence of internal waves in the GATE area suggests generation by tidal flow over topography. The intensity of the observed waves so far away from the seamounts suggests that an amplification mechanism may be present between the seamount and the point of wave encounter.

In the following, I will first discuss the frequency content of internal waves generated by tidal flow over a seamount, then consider the spatial distribution of the emitted signal, especially near the surface. A simple analysis for an idealized density and mean velocity structure then follows, and results are discussed in terms of directionality and convergence of wave propagation of the internal wave field in the upper thermocline.

2. Generation of internal waves by tidal flow over topography

Oscillatory flow over a seamount will generate waves that, at a distance from the mount, will have sufficiently small amplitudes to be treated adequately in terms of linear theory. Near the surface of the seamount, nonlinear processes (especially in the boundary layer) will be important. The boundary layer formed during one tidal cycle will persist into the next tidal cycle, leading to the continuous presence of a bottom-mixed layer. This layer will be modified in each tidal cycle. Since the inertial period at the latitudes of the GATE area

[1] A GATE paper.

(10° N) is near 70 h and the semidiurnal lunar tidal period is approximately 12.4 h, the flow will be strongly affected by the nonlinear advective effects and I suggest that processes like vortex stretching can cause overturning and wave emission which, if the surface slope is right, may induce overturning further along the slope.

The processes are too complicated to describe in detail because of our lack of detailed understanding. But we can say with some assurance that there will in all likelihood be violent events in the boundary layer on the slopes of an isolated seamount. The tidal flow around the seamount outside the boundary layer will be largely two-dimensional because of the mean stratification. The horizontal vorticity in the boundary layer on the upstream side of the mount will then be stretched due to horizontal divergence. This can lead to overturning of an initially stable density stratification. Such tumbling will in turn generate small-scale waves that can propagate on the density interface between the bottom-mixed layer and the fluid above, as well as into the fluid away from the boundary layer. The further possibility of the internal waves from one location of the seamount impinging on the boundary layer elsewhere and contributing to overturning, and the possibility that there may exist finite amplitude thermohaline instabilities that may contribute, should also be mentioned.

The purpose of this listing of processes in the bottom boundary is to justify the suggestion that the wave emission from the bottom boundary over a seamount may be predominantly in the form of a burst of waves occurring some time after the tide turns. Near the edges of continental shelves this seems to be the case; the observations of internal waves travelling on the seasonal thermocline over shelf areas seem to be of packets of internal waves emitted once per tidal period (see Halpern, 1971). We shall take the emitter intensity S at the seamount surface to be periodic in time, and suggest that the time dependence may likely be a series of pulses of finite width that can be written as

$$S=\sum_{n=0}^{\infty} a_n \sin(nM_2t+\varphi_n)$$

$$\approx \sum_{n=0}^{m} \sin[(2n-1)M_2t]. \qquad (1)$$

The last expression is a sum of alternating sign pulses, their width depending on m. This ignores the presence of low-frequency oscillation in the inertial frequency range. I will just remark that the presence of lower frequency oscillations, such as inertial motions, will serve to modulate the emitter intensity as given above and possibly give nonlinear couplings between tidal and lower frequency oscillations.

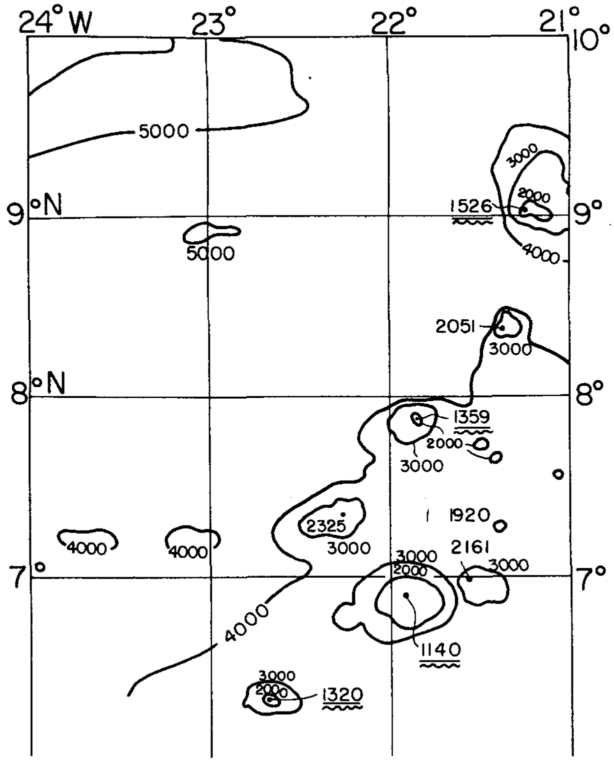

FIG. 1. Bottom topography in the GATE area. Depths in meters.

3. Propagation of waves away from the seamount

Use will be made of a linear approximation to discuss the propagation of waves into the region surrounding the seamount. We shall discuss the propagation for an ocean with constant Brunt-Väisälä frequency. Rao (1975) has given the singular solution for internal-inertial waves generated by an oscillatory vertical point force in an infinite fluid both with and without the Boussinesq approximation. In both cases, the solutions are singular along the characteristic cones given by

$$(x^2+y^2)/z^2=(N^2-\sigma^2)/(\sigma^2-f^2), \qquad (2)$$

where σ is the frequency. Although we don't know the source strength, we can still discuss some of the consequences of seamount geometry upon the distribution of wave intensity near the sea surface. Fig. 1 shows the bottom topography in a portion of the GATE area and Fig. 2 the cross section of the seamount near 8°N, 20°W. Also shown are the characteristic slopes from the edge of the seamount plateau assuming a constant Brunt-Väisälä frequency of 2π per hour.

Fig. 2 also indicates how the characteristic surfaces will be modified for a more realistic stratification, where the Brunt-Väisälä frequency increases towards the sea surface to the bottom of the mixed surface layer.

Fig. 3 illustrates the effect of convexity of isobaths on wave intensity near the surface. The characteristic cones from, say, a circular line of emitters will give a

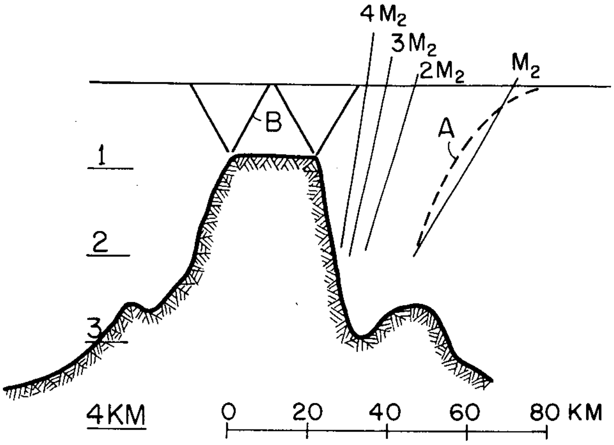

FIG. 2. Cross section of seamount near 7°N, 22°W. Characteristic slopes are shown for frequencies equal to the first four harmonics of the semidiurnal tidal frequency M_2, for constant Brunt-Väisälä frequency. Modification of characteristic slope is suggested by A; characteristic cones from edges of seamount plateau are shown at B.

maximum intensity along the envelope of the circles that represent the intersections of characteristic cones with the sea surface. In summary, we conclude that waves are emitted from the bottom-mixed layer periodically each tidal cycle, and the convergence of waves emitted from different areas of the seamount surface is in all likelihood an important factor in determining the distribution of wave intensity near the sea surface.

4. Planar wave impinging on moving surface layer

In order to demonstrate the possibility of amplification when waves from a seamount hit a moving surface layer, consider the simple mean stratification shown in Fig. 4. An upper, homogeneous layer of thickness H is moving at constant velocity U in the x direction. Below the water is at rest in the mean and has a constant Brunt-Väisälä frequency N. A simple harmonic planar wave travelling with positive upward group velocity

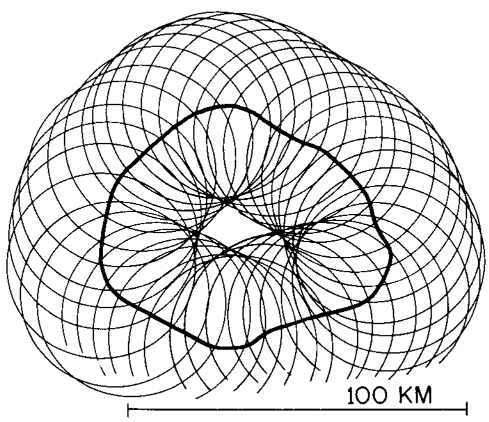

FIG. 3. Top view of characteristic cones from edges of seamount plateau where they intersect the sea surface.

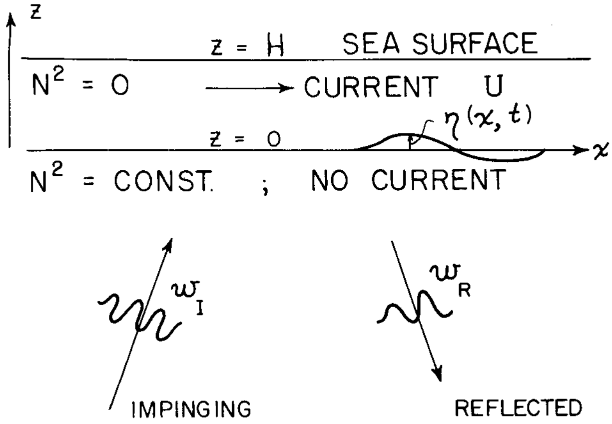

FIG. 4. Mean stratification and velocity field for model. Impinging and reflected waves also indicated.

impinges on the bottom of the mixed layer, generating a disturbance in the surface layer and a reflected wave travelling with a downward group velocity in the water below the thermocline. We have also taken the density difference across the lower interface of the mixed surface layer to be nonzero, equal to $\Delta\rho$.

a. Equation of motion

We shall use the Boussinesq approximation on an f plane, let the subscripts x, y, z, t denote partial derivatives, and define the linear convective operator D and the horizontal Laplacian, respectively, as

$$D \equiv \partial/\partial t + U\partial/\partial x, \tag{3}$$

$$\nabla_H{}^2 \equiv \partial^2/\partial x^2 + \partial^2/\partial y^2. \tag{4}$$

The linear approximations to the momentum, continuity and density equations are

$$Du - fv + P_x = 0 \tag{5}$$

$$Dv + fu + P_y = 0 \tag{6}$$

$$Dw + P_z + g\rho'/\rho_0 = 0 \tag{7}$$

$$u_x + v_y + w_z = 0 \tag{8}$$

$$D\rho' + w\bar{\rho}_z = 0. \tag{9}$$

From these equations one obtains the equation of vertical vorticity:

$$D\zeta = D(v_x - u_y) = fw_z. \tag{10}$$

Eqs. (5) and (6) yields the pressure equation

$$\nabla_H{}^2 P = Dw_z + f\zeta, \tag{11}$$

while Eqs. (7) and (9) give

$$-DP_z = (D^2 + N^2)w. \tag{12}$$

Combining Eqs. (10) and (12) gives

$$(N^2 + D^2)\nabla_H{}^2 w + (f^2 + D^2)w_{zz} = 0. \tag{13}$$

b. The impinging and reflected waves

If we take the disturbances in the lower fluid to consist of an impinging wave w_I and a reflected wave w_R given by

$$w_I(x,y,z,t)=\hat{W}_I \exp[i(-\gamma z+kx-\sigma t)], \qquad (14)$$

$$w_R(x,y,z,t)=\hat{W}_R \exp[i(+\gamma z+kx-\sigma t)], \qquad (15)$$

Eq. (13) gives the dispersion relation

$$\gamma^2=k^2(N^2-\sigma^2)/(\sigma^2-f^2), \qquad (16)$$

where we take γ to be positive so as to give the proper directions of group velocities.

The associated pressure fields are

$$\hat{P}_I=(N^2-\sigma^2)\hat{W}_I/(\sigma\gamma), \qquad (17)$$

$$\hat{P}_R=-(N^2-\sigma^2)\hat{W}_R/(\sigma\gamma). \qquad (18)$$

The kinematic boundary condition at the lower interface of the mixed layer is

$$\hat{W}_I+\hat{W}_R=-i\sigma\hat{h}, \qquad (19)$$

where $\hat{h}$ is the complex amplitude of the interface between the upper layer and the fluid below, as defined in (20).

c. Disturbance in the upper layer

If we express the vertical velocity field and pressure in terms of the deflection of the interface at the bottom of the moving layer $z=h(x,t)$, taking

$$h(x,t)=\hat{h}\exp[i(kx-\sigma t)], \qquad (20)$$

the kinematic boundary condition at the interface $z=h(x,y,t)$ is

$$w_u(x,0,t)=Dh.$$

This condition is satisfied by setting

$$w_u(x,0,t)=-i\omega\hat{h}\exp[i(kx-\sigma t)], \qquad (21)$$

where

$$\omega=\sigma-Uk. \qquad (22)$$

Since the upper fluid is homogeneous, $N^2=0$, and a solution to Eq. (13) that also satisfies the boundary condition of zero vertical velocity at the free surface $z=H$ as well as the kinematic condition at $z=0$ is

$$w_U(x,z,t)=(i\omega\hat{h}/\sinh\alpha H)\sinh\alpha(z-H) \times\exp[i(kx-\sigma t)]. \qquad (23)$$

The associated pressure field is found from Eq. (11) which gives (after some algebra)

$$P_U(x,z,t)=[-\omega^2/(\alpha\sinh\alpha H)]\hat{h}\cosh\alpha(z-H) \times\exp[i(kx-\sigma t)], \qquad (24)$$

where

$$\alpha^2=k^2\sigma^2/(\sigma^2-f^2), \quad f^2<\sigma^2<N^2. \qquad (25)$$

d. Pressure matching at z=0

We let $g'=g\Delta\rho/\rho_0$. The pressure matching condition across the density interface between the upper and lower fluids is

$$P_I+P_R=P_U+g'h \quad \text{at} \quad z=0. \qquad (26)$$

Using Eqs. (14)–(17), this can be written

$$\hat{W}_I-\hat{W}_R=\gamma\sigma\hat{h}[-(\omega^2/\alpha)\coth\alpha H-g'](N^2-\sigma^2)^{-1}, \qquad (27)$$

which, taken with Eq. (19), will allow one to solve for the amplitudes of the reflected wave and the surface layer disturbance in terms of the amplitude w_I of the impinging wave. Adding Eqs. (19) and (26), one finds

$$2\hat{W}_I=\sigma\hat{h}\{-i+\gamma[g'-(\omega^2/\alpha)\coth\alpha H]/(N^2-\sigma^2)\}. \qquad (28)$$

This further gives

$$\sigma\hat{h}/(2\hat{W})=\{-i+k(N^2-\sigma^2)^{-\frac{1}{2}}(\sigma^2-f^2)^{-\frac{1}{2}} \times[g'-(\omega^2/\alpha)\coth\alpha H]\}^{-1}. \qquad (29)$$

The response of the interface is proportional to the inverse of the expression in the braces in Eq. (19). When that expression is zero, there will be an infinite response to a finite excitation and a finite response to infinitesi-

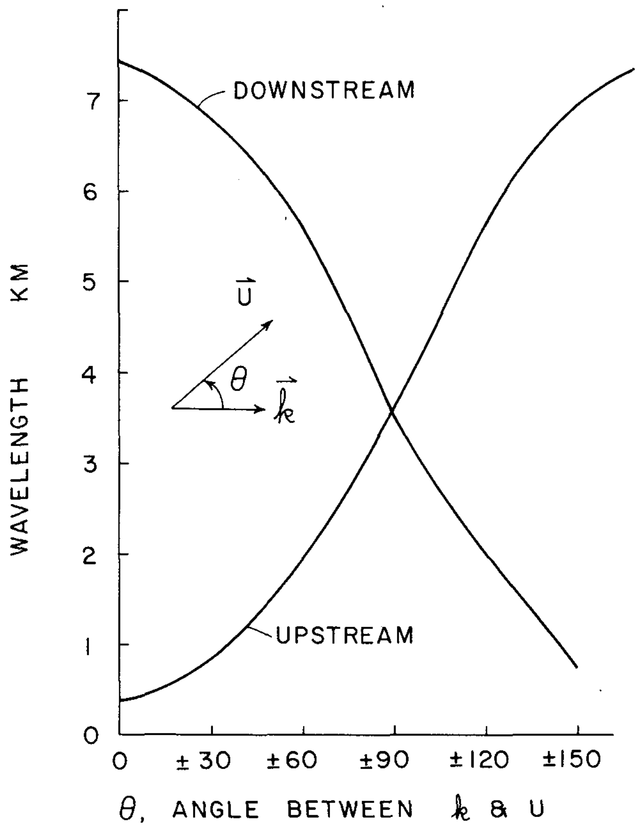

FIG. 5. Plot of maximally amplified wavelengths versus angle between surface current and horizontal wavenumber component. Two wavelengths are shown for each angle, one for waves against the current, the other for waves with the current.

mal excitation, corresponding to resonance. This then implies that the flow is neutrally stable to disturbances of corresponding wavenumber and frequency.

The GATE observations, cited below, show the presence of especially strong signals near tidal and inertial frequencies. Therefore, we first consider disturbances in the tidal frequency range, where the approximation

$$\sigma^2 \gg f^2$$

will be used. At the latitude of the GATE experiment, $\sim$10°N, the inertial period is approximately 70 h, compared to the semidiurnal lunar tidal period of 12.4 h, and the approximation made by neglecting f^2/σ^2 implies errors of order 3% in the approximated terms in Eq. (29).

The response amplitude will be a maximum when the expression in the braces is a minimum. As long as the second term in the braces is real, the maximum response will occur when the second term is zero, i.e., when

$$\omega^2 = g'\alpha \tanh \alpha H. \quad (30)$$

The amplification ratio, as defined by the left-hand side of Eq. (29), will then equal 2. For long waves, for which $kH \gg 1$, one then finds

$$\sigma/k = U \pm (g'H)^{\frac{1}{2}}. \quad (31)$$

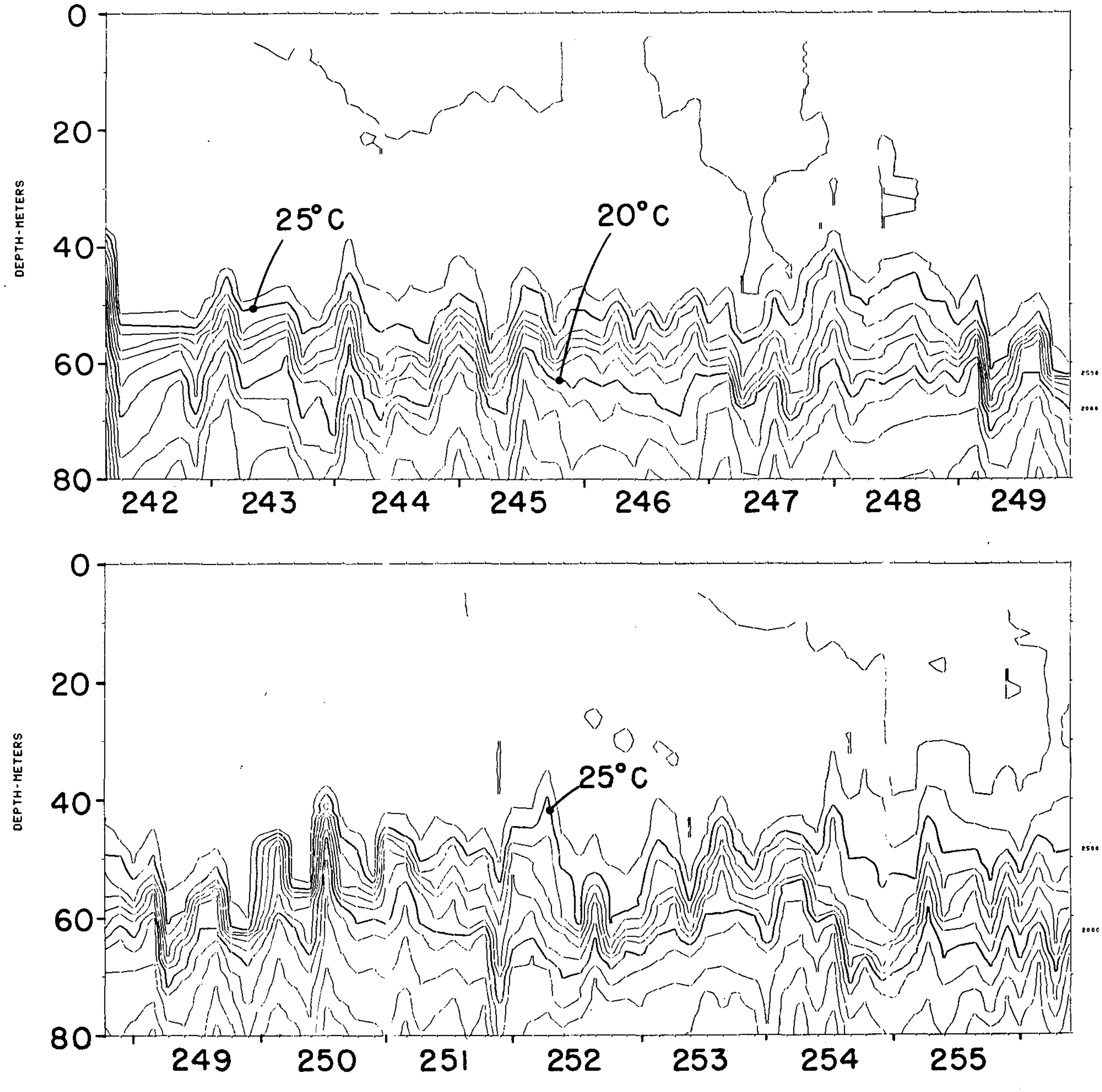

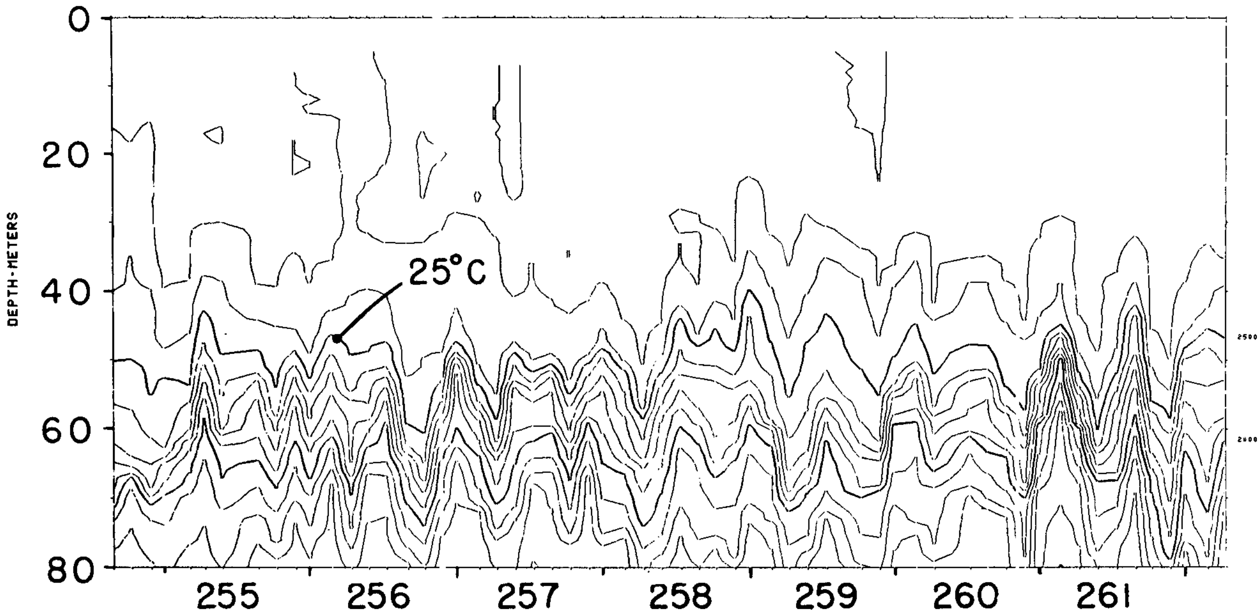

FIG. 6. Isotherm depth versus time based on data from R.V. *Oceanographer*. The sudden dip in isotherm depth occurring once per tidal period is evident. Numbers along the abscissa designate Julian day in 1974. Plot provided by P. Grose, NOAA Environmental Data Service.

The result in Eq. (31) is expressed as the wavelength of the most amplified wave of a given frequency σ as a function of the mean current speed U, the mixed layer depth H, and density contrast in Eq. (32).

For a current oblique to the horizontal component of the wavenumber of the impinging wave, only the current velocity component $U\cos\theta$ along the horizontal wavenumber direction will count. Eq. (31) then becomes

$$\lambda = 2\pi/k = [U\cos\theta \pm (g'H)^{\frac{1}{2}}]/\sigma. \quad (32)$$

Fig. 5 shows the maximally amplified wavelength as function of angle θ, calculated for lunar semidiurnal tidal frequency, a mixed layer depth of 30 m, a current velocity of 0.5 m s^{-1} and a density contrast of $\Delta\rho/\rho = 10^{-2}$. These values are typical of the GATE area.

For the other frequency range of interest, near the inertial frequency, we set $\sigma = f(1+\nu)$ and assume $|\nu| \ll 1$ in Eq. (29). Setting the braces in Eq. (29) equal to zero and neglecting terms of order ν^2, we find the response is infinite when

$$i\nu \approx g'k(N^2 - f^2)^{-\frac{1}{2}}/(f2^{\frac{1}{2}}). \quad (33)$$

This corresponds to an instability being excited by the impingement of waves at inertial frequency, since the response is a disturbance growing exponentially with time. This corresponds to a result found by Stern (1977).

5. Observations

Isotherm depths versus time, as calculated from the casts taken from R. V. *Oceanographer*, are shown in Fig. 6. The dip in isotherm depths once per tidal period is evident; the fluctuations at inertial frequency, with period of ~70 h, are less obvious.

6. Discussion

The analysis of a simplified problem, analogous to that of the impingement of topographically generated waves from below upon the moving homogeneous surface layer, shows that for frequencies well above inertial frequency the surface layer disturbance will be twice the amplitude of the impinging wave for certain wavenumbers, depending upon direction of propagation relative to the current. For waves very near inertial frequency, there can be excitation of exponentially growing disturbances, corresponding to the excitation of an instability. This singular reflection will generate waves that will propagate downward and be reflected from the bottom, to impinge again and excite instability further. This process was pointed out by Lindzen (1974) for the case of internal waves. The process is similar to the phenomenon of overreflection of sound waves from a compressible flow shear layer, analyzed by Landau (1944), and later by Miles (1957) and by Ribner (1957). The importance of spatially growing disturbances when there is a solid boundary or a second shear layer present was pointed out by Mollo-Christensen (1959) for the acoustic case.

The analysis given here, even if the problem has been very much simplified to render it tractable, seems to suggest the processes that contribute to the generation of disturbances in the upper ocean have significant energy at tidal frequency and its harmonics, as well as at the inertial frequency.

Another possibly important conclusion of the discussion of wave emission from topography is the effect of isobath convexity on the convergence of topographic waves impinging on the sea surface; the waves may, through convergence, attain sufficient amplitude to generate surface waves through nonlinear interactions, although no observations have been reported.

In conclusion we may state that the internal waves observed in the GATE experiment may have been generated by tidal flow over topography, as suggested by Ostapoff *et al.* (1975).

Acknowledgments. The work reported in this paper was supported by the Office of Naval Research under Contract N00014-75-C-0291. I also acknowledge the very helpful suggestions of the reviewer of an earlier version of this paper.

REFERENCES

Apel, J. R., H. M. Byrne, J. R. Proni and R. L. Charnell, 1975: Observations of oceanic internal waves from the Ocean Resource Technology Satellite. *J. Geophys. Res.*, **80**, 865–881.

Halpern, D., 1971: Semidiurnal internal tides in Massachusetts Bay. *J. Geophys. Res.*, **76**, 6573–6584.

Koblinsky, C., and P. L. Grose, 1975: Anomalous variations in *T-S* relationships at GATE station 7. GATE Rep. No. 14, 368–371.

Landau, L., 1944: Stability of tangential discontinuities in compressible fluids. *CR Acad. Sci. USSR*, **44**, No. 4, 139–141.

Lindzen, R. S., 1974: Stability of a Helmholz profile in a continuously stratified Boussinesq fluid—applications to clear-air turbulence. *J. Atmos. Sci.*, **31**, 1507–1514.

Miles, J. W., 1957: On the reflection of sound at the interface of relative motion. *J. Acoust. Soc. Amer.*, **29**, 226–228.

Mollo-Christensen, E. (1959): Acoustical instability of jets and wakes for Mach numbers above two. *J. Aero/Space Sci.*, **26**, 765–766.

——, K. A. Morey and D. Strimaitis, 1975: Towed probe observations made from R. V. Columbus Iselin during GATE. Tech. Rep., Contract DES 71-00324, Dept. of Meteorology, MIT.

Ostapoff, F., J. R. Proni and R. Sellers, 1975: Preliminary analysis of ocean internal wave observations by acoustic soundings. GATE Rep. No. 14.

Phillips, O. M., 1966: *Dynamics of the Upper Ocean.* Cambridge University Press, 261 pp.

Rao, A. R., 1975: On an oscillatory point force in a rotating stratified fluid. *J. Fluid Mech.*, **72**, 353–362.

Rattray, M., 1960: On the coastal generation of internal tides. *Tellus*, **12**, 54–62.

Ribner, H. S., 1957: Reflection, transmission and amplification of sound by a moving medium. *J. Acoust. Soc. Amer.*, **29**, 435–445.

Siedler, G., and W. Zenk, 1975: Variations of temperature, salinity and currents in the mixed layer and thermocline (preliminary results). GATE Rep. No 14.

Stern, M. E., 1977: Interaction of inertia waves with wind. *J. Mar. Res.* (in press).

Woods, J. D., 1975: Batfish experiments during Phase III of GATE. Unpubl. manuscript, Oceanography Department, University of Southhampton, U. K.